Proceedings of the International Symposium on Engineering Lessons Learned from
the 2011 Great East Japan Earthquake, March 1-4, 2012, Tokyo, Japan

SEISMIC RESPONSE ANALYSIS OF A SEMI-ACTIVE-CONTROLLED BASE-ISOLATED BUILDING DURING THE 2011 GREAT EAST JAPAN EARTHQUAKE

Kosuke NAKAJIMA[1], Nicolas GIRON[1], Masayuki KOHIYAMA[1],
Keisuke WATANABE[1], Minako YOSHIDA[1], Masayuki YAMANAKA[2],
Satoru INABA[2], and Osamu YOSHIDA[2]

[1] Graduate School of Science and Technology, Keio University, Kanagawa, Japan,
na6061ko6041@z7.keio.jp
[2] Obayashi Corporation, Minato-ku, Tokyo, Japan

ABSTRACT:
The dynamic properties are examined for a university building with a semi-active base isolation system during the 2011 Great East Japan earthquake. First, the natural periods, damping factors, and mode shapes are identified using an ARX model and the N4SID method based on the observation records of the main shock of this earthquake, in which the building performed as a passive base isolation system due to a maintenance work. Then, the stiffness and damping coefficients of the building are identified using the same records. Finally, the performances of the semi-active base isolation system are analyzed using an aftershock record based on a response simulation of the identified model.

Key Words: base isolation system, Great East Japan earthquake, system identification, semi-active control

INTRODUCTION

Sousoukan, a nine-story university building at Keio University, which was completed in 2000, has a semi-active base isolation system (Yoshida 2001). During the 2011 Great East Japan earthquake, the semi-active system was not in service due to a maintenance work, and the building performed as a passive base isolation system. When the main shock of the earthquake occurred on March 11, 2011, numbers of engineers worked in the base isolation layer for the inspection of the semi-active base isolation system; fortunately, none of them were injured. Only slight damage was found in a bridge between Sousoukan and a neighboring RC building etc, and thus the response of the building seems to be effectively reduced by the base isolation system. It should be noted that falling of stored contents were not reported in the building whereas it was observed in an adjacent library building.

This paper focuses on the identification of dynamic properties of the system using the data collected during the Great East Japan earthquake. Three types of system identification methods were employed, an ARX mode (Mita 2003), the N4SID method (Van Overschee and De Moor 1994), and a

direct optimization method of structural parameters to minimize an error in a response time history (hereafter Direct method). The natural periods and damping factors of the system are identified and the structural parameters, i.e. stiffness and damping coefficients, are updated from those assumed in design. As the amplitude and the duration of this earthquake are abnormally important, the accuracy of the identification is improved by neglecting measure noises and using the large available quantity of data.

Then, using the identified model, the performance of the semi-active base isolation system is analyzed based on a response simulation with based on a record of an aftershock of April 7, 2011, during which the semi-active system is considered to be activated.

BUILDING INFORMATION

Figure 1 shows the section views of Sousoukan. The locations of the isolation bearings are depicted in the left diagram. The isolation layer is composed of 65 laminated rubber bearings, 24 passive hydraulic dampers and 8 semi-active dampers. The damping coefficient of the semi-active dampers can be switched between four stages. The right diagram shows the framing system of the building, which consists of steel, steel reinforced concrete and concrete filled steel tube. The building has nine layers: seven floors above the ground and two basement floors. The short side direction of the building is shifted with 25 degrees from the north-south direction as shown in Fig. 1. In this paper, however, we call the short side direction as the NS direction.

There are two independent seismic observation systems in the building: one is for control of the semi-active system and the other is for research. The accelerometers are placed at the foundation slab, the 2nd basement, the 1st and the 7th floors as well as the ground near the building. Design structural parameters are presented in Table 7 of the appendix.

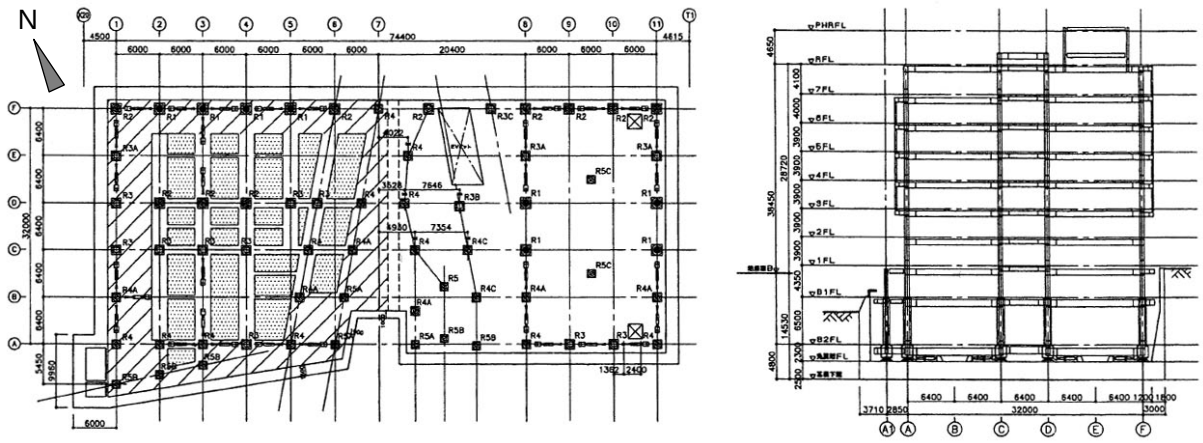

Fig. 1 Section views of Sousoukan

ESTIMATION OF DYNAMIC PROPERTIES WITH ARX MODEL AND N4SID METHOD

First, we estimated the 1st and 2nd natural periods, natural frequencies and damping factors of the entire building and the superstructure of the building from the accelerograms of the main shock (Fig. 2) using an ARX model. The acceleration records at the foundation slab are used as input, and those at the 7th floor as output. The acceleration records between 100 and 150 s, in which large amplitude of the principal shock is observed, are used for the estimation. The number of poles, the number of zero points, and dead time are set to 12, 4, and 1 respectively. In the analysis, all the accelerograms and other records are filtered by a third order Butterworth high pass filter with a cut-off frequency of 0.125 Hz considering causality. Tables 1 and 2 show the identified results for the entire building and the

superstructure, respectively.

Then, the 1st and 2nd natural frequencies and damping factors of the entire building are also identified using the N4SID method. The acceleration records at the foundation slab were employed for input, and those of the 2nd basement, the 1st floor, and the 7th floors for output. The acceleration records of three time windows: between 20 and 60 s, between 100 and 150 s (the principal shock), and between 200 and 300 s, were used for estimations. The dimension of the state space model was 18 for the EW direction and 17 for the NS direction. The identified results are shown in Table 3. Similarly, the 1st and 2nd natural frequencies and damping factors of the superstructure of the building were estimated; the dimension of the state space model is 18 for the EW direction and 16 for the NS direction. The identified results are shown in Table 4. The mode shapes are depicted in Fig. 3.

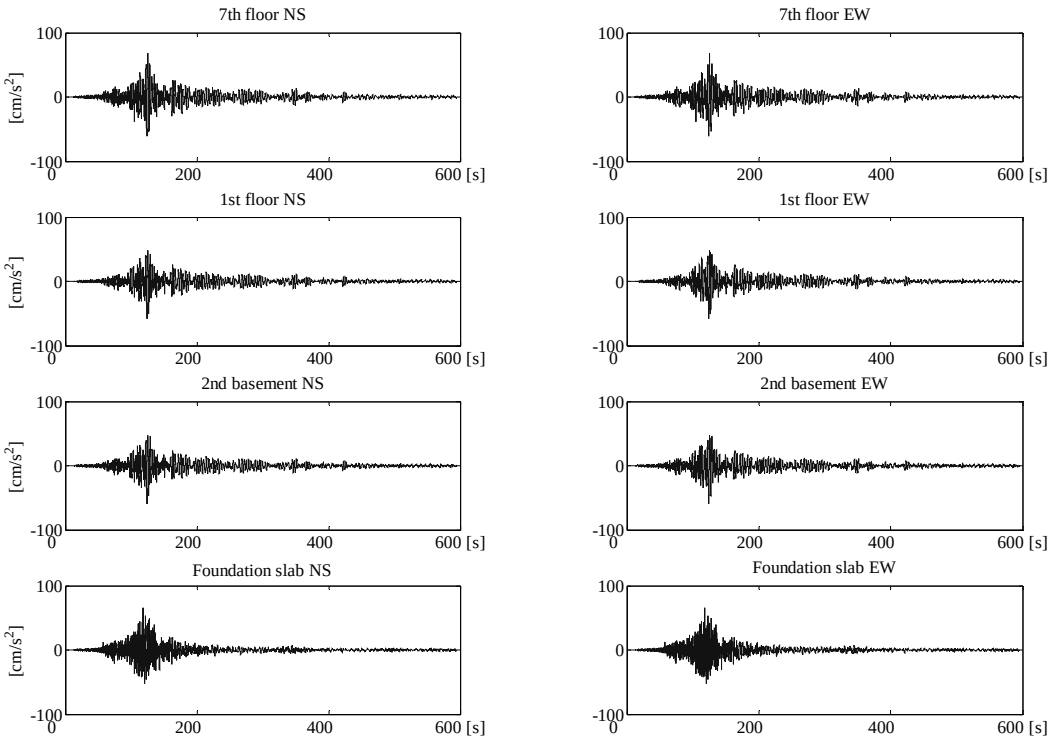

Fig. 2 Observed records of the main shock

Table 1 Estimated system parameters for the entire building based on an ARX model

Direction	Mode	Natural period [s]	Natural frequency [Hz]	Damping factor
NS direction	1st	3.2	0.31	0.19
	2nd	0.68	1.5	0.17
EW direction	1st	3.1	0.32	0.24
	2nd	0.71	1.4	0.16

Table 2 Estimated system parameters for the superstructure of the building based on an ARX model

Direction	Mode	Natural period [s]	Natural frequency [Hz]	Damping factor
NS direction	1st	1.1	0.91	0.05
	2nd	0.36	2.8	0.08
EW direction	1st	1.1	0.91	0.022
	2nd	0.37	2.7	0.04

Table 3 Estimated system parameters of the entire building based on the N4SID method

Direction	Mode	Natural Frequency [Hz]			Damping factor		
		20-60 s	100-150 s	200-300 s	20-60 s	100-150 s	200-300 s
NS direction	1st	0.48	0.31	0.32	0.141	0.180	0.132
	2nd	1.66	1.42	1.49	0.110	0.0626	0.303
EW direction	1st	0.48	0.31	0.32	0.263	0.166	0.158
	2nd	1.46	1.38	1.41	0.110	0.0760	0.0782

Table 4 Estimated system parameters of the superstructure of the building based on the N4SID method

Direction	Mode	Natural Frequency [Hz]			Damping factor		
		20-60 s	100-150 s	200-300 s	20-60 s	100-150 s	200-300 s
NS direction	1st	1.13	0.86	0.83	0.043	0.019	0.050
	2nd	2.15	2.12	2.91	0.036	0.067	0.057
EW direction	1st	1.04	0.90	0.83	0.037	0.081	0.040
	2nd	2.70	2.51	2.70	0.024	0.099	0.053

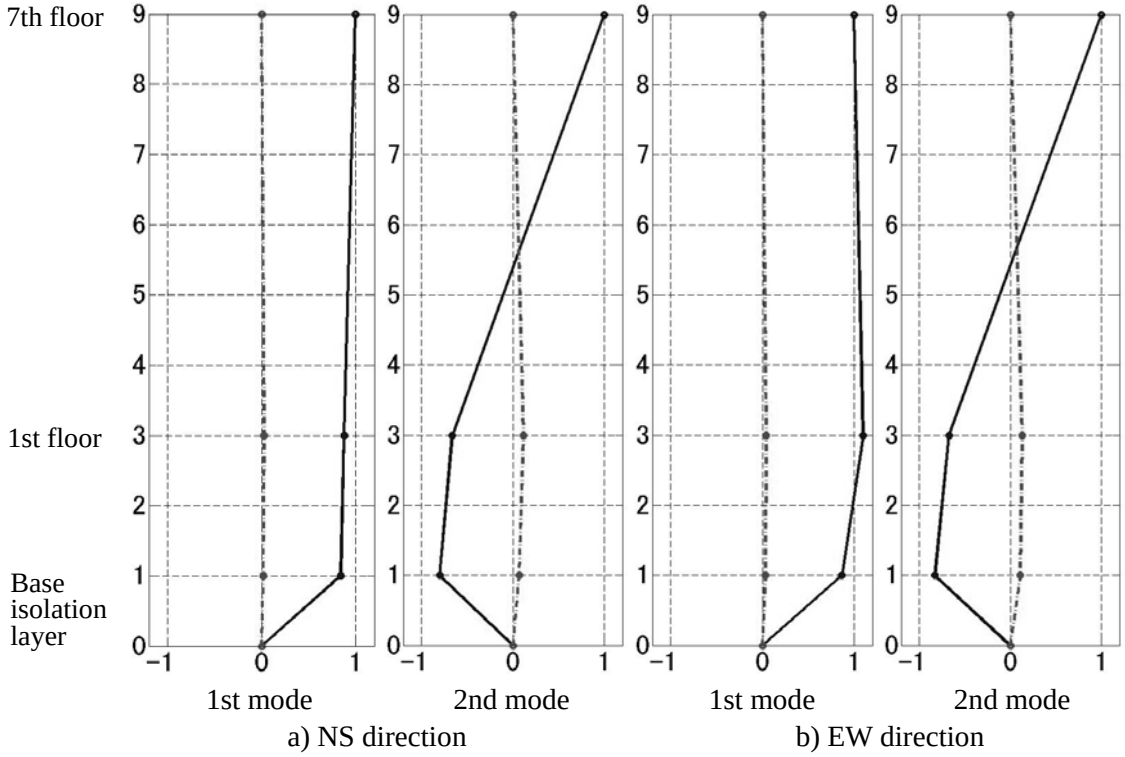

Fig. 3 Estimated 1st and 2nd mode shapes for the time interval from 100 to 150 s (solid: real, dashed: imaginary)

RESTORING FORCE PROPERTIES OF THE ISOLATION LAYER

The restoring force properties of the isolation layer are calculated. Since relative displacements records were not measured in the main shock, the relative displacements of the isolation layer are derived based on acceleration records at the foundation slab and the 2nd basement floor using double integral and a Butterworth filter considering causality. The Lissajous figure of the relative displacements of the isolation layer is indicated in Fig. 4.

The restoring force is approximated by the acceleration at the 2nd basement floor multiplied by the mass of the superstructure. The Figs. 5 and 6 describe the restoring forces for every 10 seconds. The degradation of stiffness is observed after and before the principal shock.

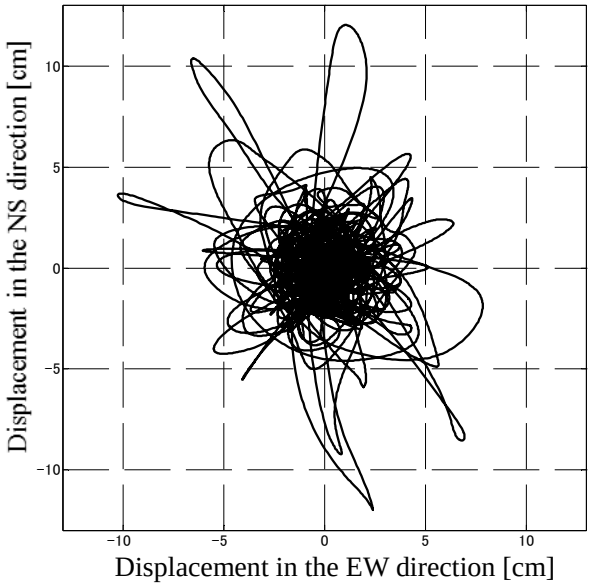

Fig. 4 Lissajous Figure

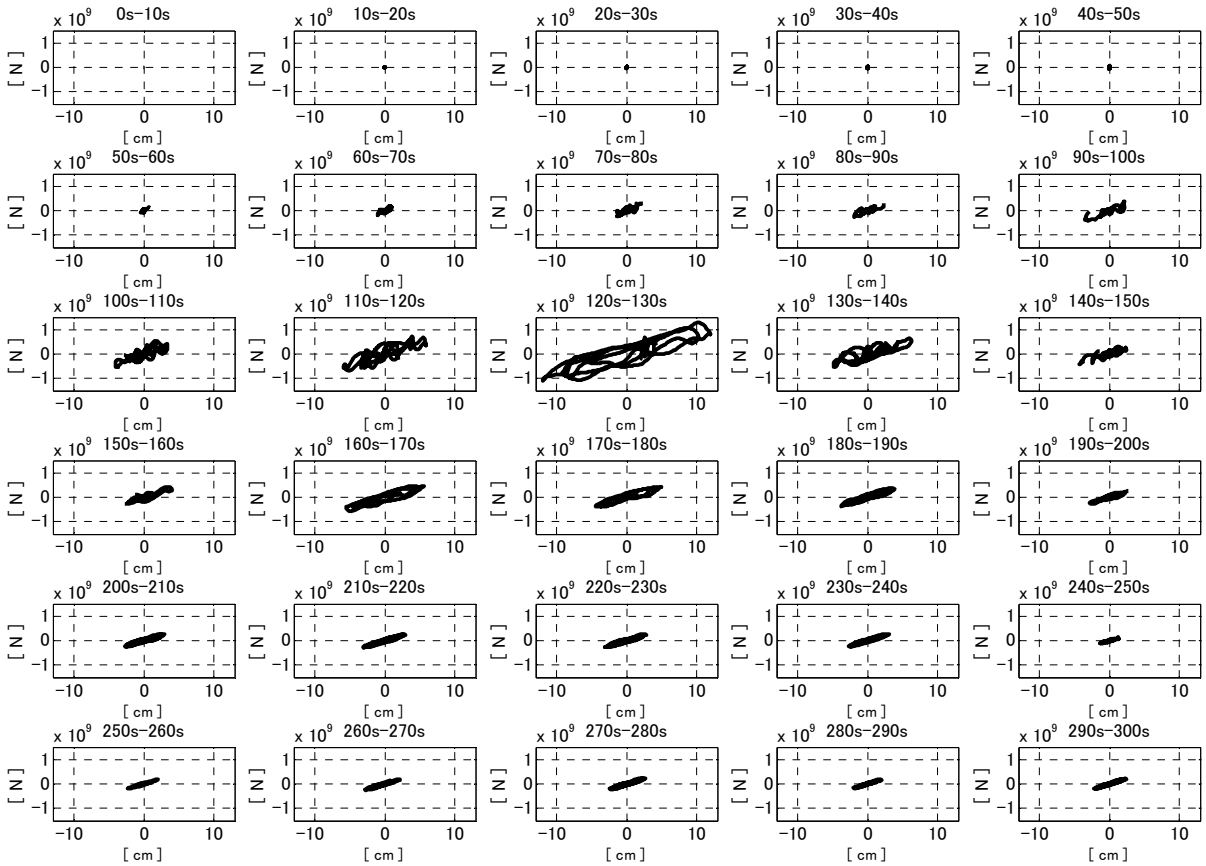

Fig. 5 Restoring force properties of the isolation layer in the NS direction

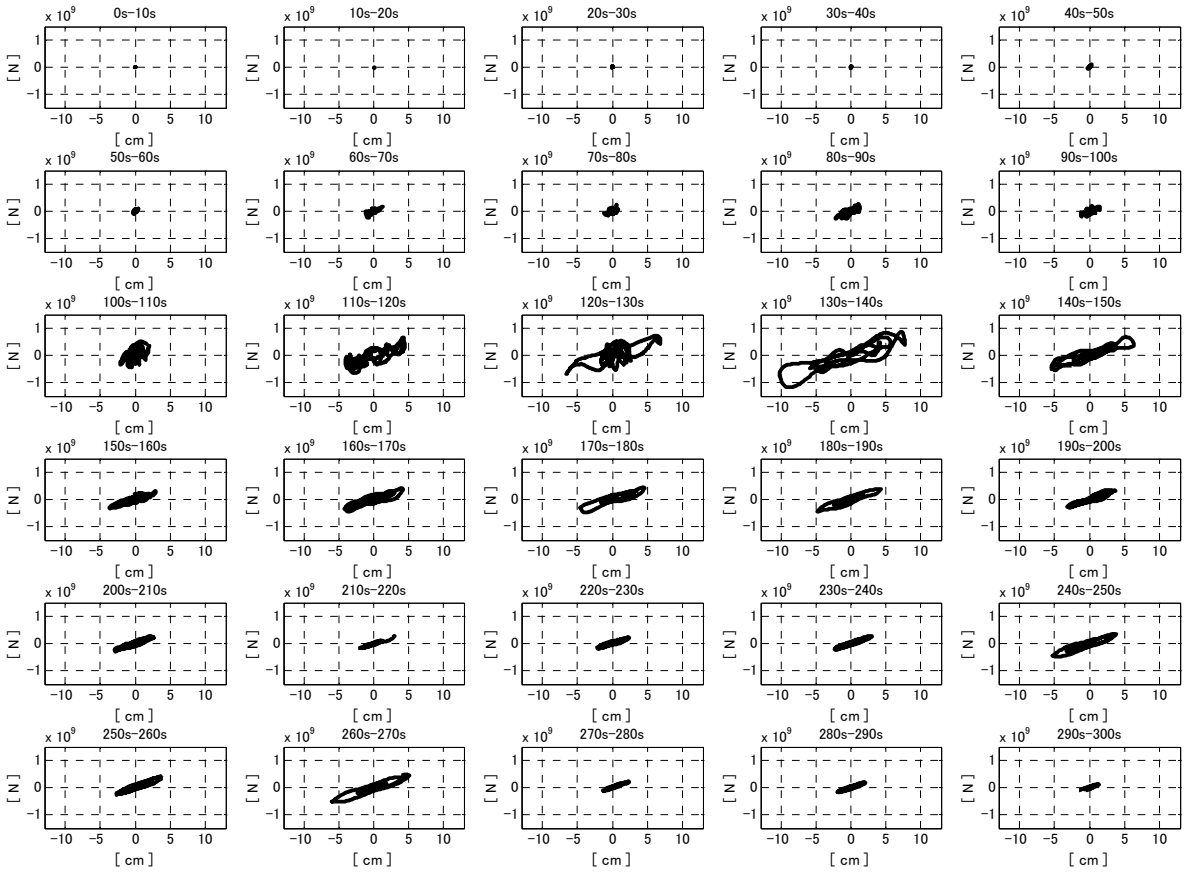

Fig. 6 Restoring force properties of the isolation layer in the EW direction

SYSTEM PARAMETERS OPTIMIZATION

By utilizing the estimated natural periods and damping ratios of the system, the structural parameters, i.e. stiffness and damping coefficients, are updated. The seismic analyses were conducted with those updated parameters and compared with the observed acceleration records.

Consideration of Maxwell Damper

Among the 32 dampers in the base isolation layer, eight of them, four per direction, are semi-active Maxwell dampers and as a consequence, to update correctly the structural parameters based on identification data, the state matrix of the system is adequately transformed.

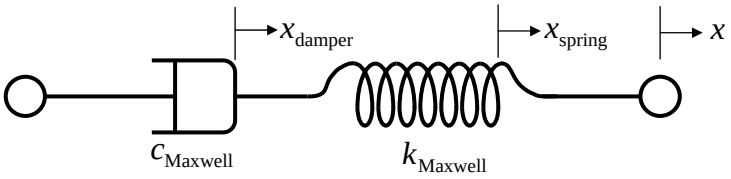

Fig. 7 Maxwell Damper

First, let consider the restoring force that corresponds to a Maxwell damper. As damper (c_{Maxwell} = 0.85, 1.7, 8, and 15 tf/kine) and spring (k_{Maxwell} = 30 tf/cm) are series, they are applied the same force F and

the total deformation x is divided between both elements leading to the following equations:

$$F = F_{\text{damper}} = F_{\text{spring}} \quad \text{and} \quad x = x_{\text{damper}} + x_{\text{spring}} \;\Rightarrow\; \dot{F} = k_{\text{Maxwell}}\dot{x} - \frac{k_{\text{Maxwell}}}{c_{\text{Maxwell}}}\, F \tag{1}$$

Considering the particular case when Maxwell dampers are only installed at the base isolation layer, the state equation of the system can be restated as:

$$\mathbf{A}\dot{\mathbf{X}} + \mathbf{B}\mathbf{X} = \begin{bmatrix} \mathbf{M} & \mathbf{O} & \mathbf{0} \\ \mathbf{O} & \mathbf{O} & \mathbf{0} \\ \mathbf{0} & \mathbf{0} & 0 \end{bmatrix} \begin{bmatrix} \mathbf{1} \\ \mathbf{0} \\ 0 \end{bmatrix} \ddot{x}_g \tag{2}$$

with

$$\mathbf{A} = \begin{bmatrix} \mathbf{O} & \mathbf{M} & \mathbf{0} \\ \mathbf{M} & \mathbf{C} & \mathbf{0} \\ \mathbf{0} & -k_{\text{maxwell}} \times \boldsymbol{\delta}_1^{\mathrm{T}} & 1 \end{bmatrix}, \quad \mathbf{B} = \begin{bmatrix} -\mathbf{M} & \mathbf{O} & \mathbf{0} \\ \mathbf{O} & \mathbf{K} & 4\boldsymbol{\delta}_1 \\ \mathbf{0} & \mathbf{0} & \dfrac{k_{\text{maxwell}}}{c_{\text{maxwell}}} \end{bmatrix} \text{ and } \quad \mathbf{X} = \begin{bmatrix} \dot{\mathbf{x}} \\ \mathbf{x} \\ F \end{bmatrix}, \quad \boldsymbol{\delta}_1 = \begin{bmatrix} 1 \\ 0 \\ \vdots \\ 0 \end{bmatrix} \tag{3}$$

where **M**, **C** and **K** are the mass, damping, and stiffness matrices, respectively; **x** and $\ddot{x}_g$ are the relative displacement vector and the ground acceleration.

Direct Identification Method

Rather than identifying the natural periods and damping ratios of the system, it is possible to directly estimate the structural parameters by defining a measure of the error e between outputs time histories of the original system **y** and the estimated system $\mathbf{y}_m$. As story masses are supposed to be correctly estimated at the design stage, and only inter story stiffness **k** and damping coefficients **c** are updated.

During strong ground motions, primary concern is given to the maximum value of drift and acceleration; thus the error e is defined to give much importance to the approximation of peak values.

$$e = \frac{1}{n_{\text{output}}} \sum_{i=1}^{n_{\text{output}}} \frac{1}{n_{\text{time}} \operatorname{mean}_j(|y_{ij}|)} \sqrt{\sum_{j=1}^{n_{\text{time}}} \left|(y_{ij} - y_{m,ij})\, y_{ij}\right|} \tag{4}$$

Consequently the values of **k** and **c** are obtained by minimizing e. This measure can also be used to compare this identification method with an ARX model and the N4SID method. The natural periods and damping ratios corresponding to the direct identification are given in appendix.

Updated Parameters

The updated structural parameters are also obtained by using the ARX and N4SID results. The update is realized by optimizing **K** and **C** matrices, so that the natural periods and damping ratios calculated from the complex eigenvalues analysis (Eq. 5) of the **A**-**B** system of Eq. (3) are similar to the results of the ARX and the N4SID identifications.

$$|\boldsymbol{\Omega}\mathbf{A} + \mathbf{B}| = 0, \quad \omega_n = |\Omega_n|, \quad \xi_n = -\operatorname{Re}(\Omega_n) / |\Omega_n| \tag{5}$$

Updated stiffness and damping coefficients are depicted on Figs. 8 and 9.

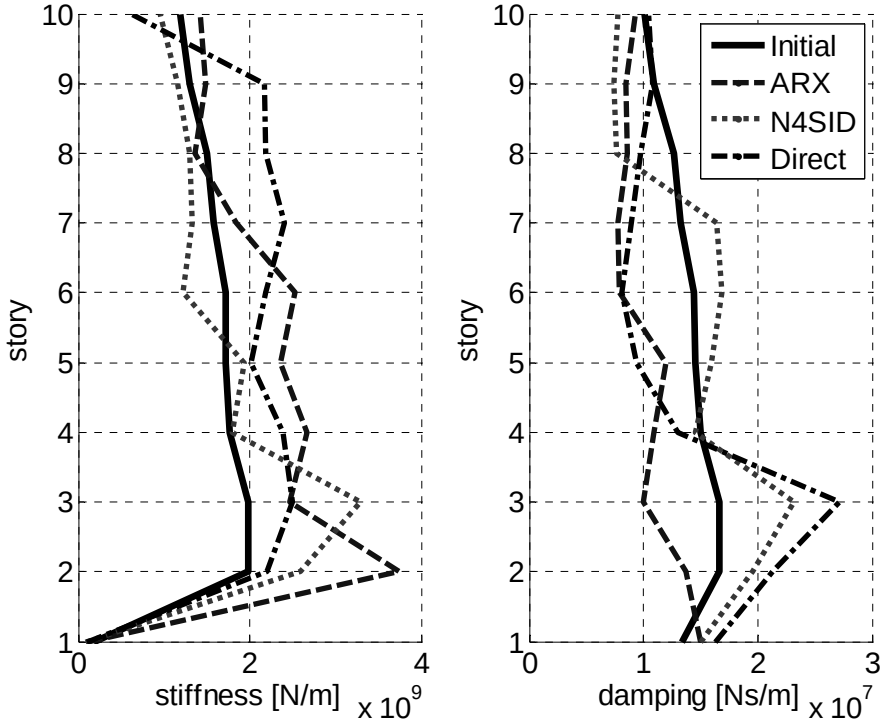

a) Stiffness b) Damping

Fig. 8 Updated stiffness and damping coefficients in the NS direction

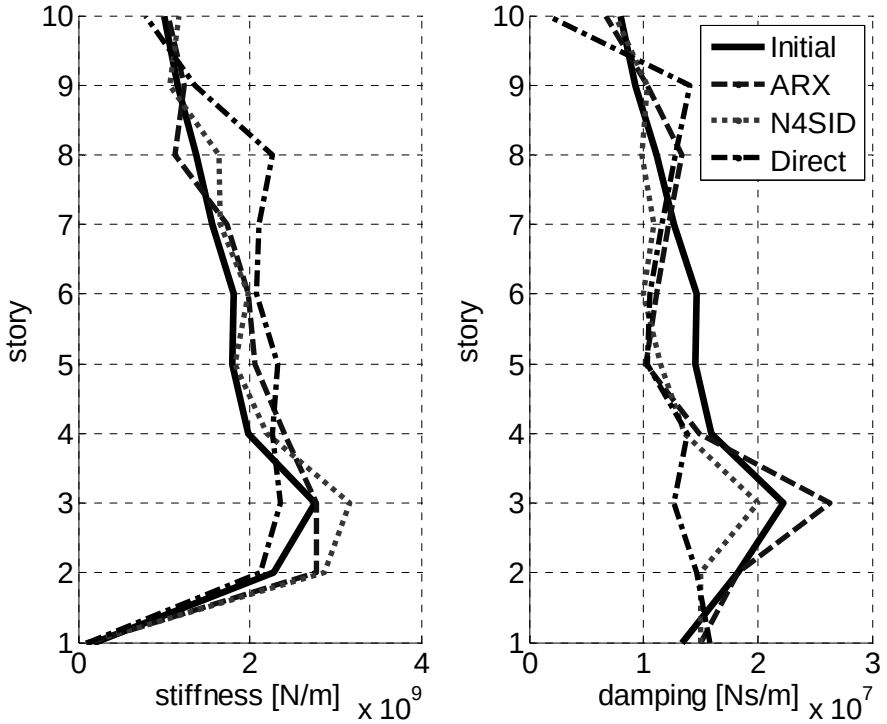

a) Stiffness b) Damping

Fig. 9 Updated stiffness and damping coefficients in the EW direction

Seismic Response Analysis

Seismic response analyses with updated structural parameters are conducted for two seismic events: the main shock and the aftershock that occurred 30 minutes later. The acceleration response spectra of the records observed at the foundation slab are shown in Fig. 10.

All three identifications are realized using the main shock data and their accuracy is checked using the aftershock data. Considering the identification measure error *e*, the three methods are compared and the results are summarized in Table 5. Also, a time history portion is displayed in Fig. 11 to figure out the accuracy of identification. According to those results, the direct identification method gives the best and most robust approximation; however, the computation time is more extensive.

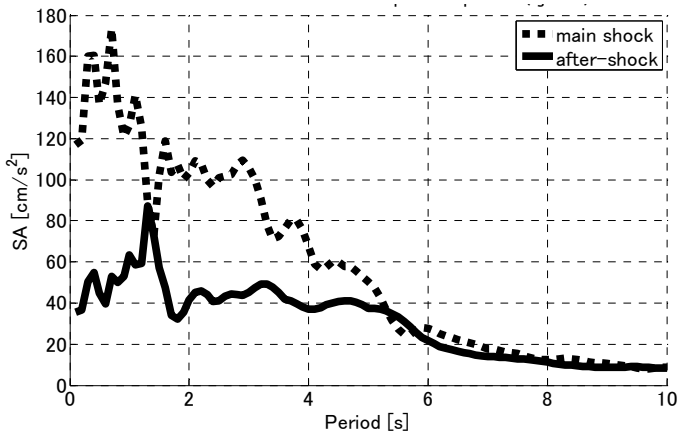

a) NS direction

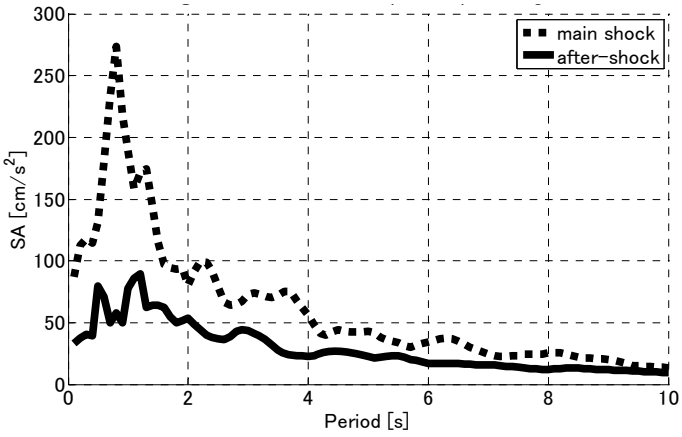

b) EW direction

Fig. 10 Acceleration response spectra of the main shock and the 30-minute-later aftershock

Table 5 Error *e*

Identification Method	Main Shock		Aftershock	
	NS direction [10^{-3}]	EW direction [10^{-3}]	NS direction [10^{-3}]	EW direction [10^{-3}]
Initial	6.3	5.4	7.5	5.3
ARX	2.9	2.8	2.9	2.3
N4SID	4.6	3.3	5.9	3.1
Direct	2.8	2.2	3.1	2.1

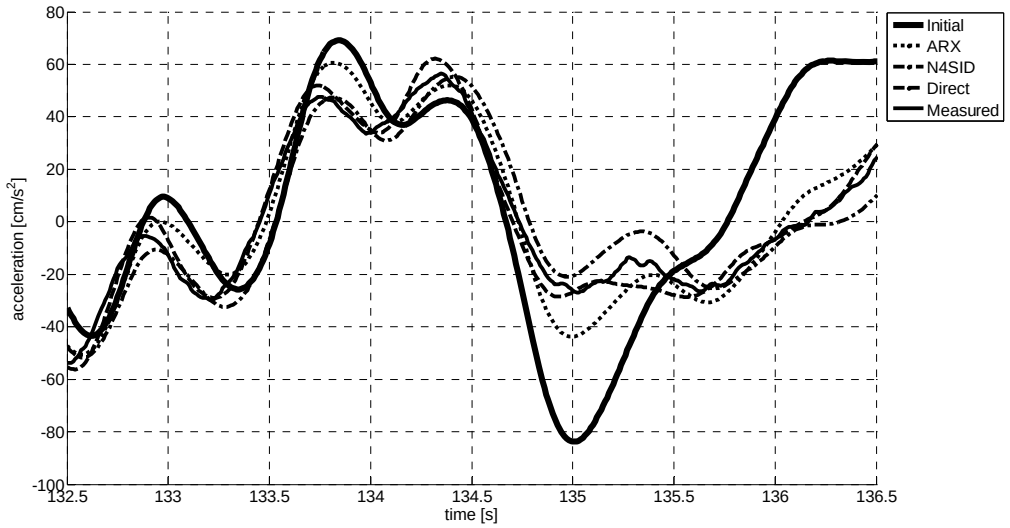

Fig. 11 Comparison of time histories for the main shock 7F EW direction

SEMI-ACTIVE SYSTEM

The semi-active system control force is derived by the LQG theory and then divided into four damping coefficient gains for the Maxwell damper. Figure 12 shows time history of the damping coefficient calculated from the record of the control signal during the April 7, 2011 aftershock. As the LQG theory relies on structural parameters of the building to be controlled, the results obtained through the previous identifications are expected to improve significantly the system response. However, at the time of this study, only performances of the control method using the structural parameters at design stage are evaluated. The simulation results are compared among three control cases: 1) the lowest damping coefficient is given to the semi-active dampers (passive low), 2) the highest damping coefficient is given to them (passive high), and 3) the time history of the damping coefficient shown in Fig. 12 is applied to them (semi-active).

The results for the aftershock are summarized in Table 6 and Fig. 13. Globally, the semi-active control gives the best performances; however, the difference with the passive control is very small and thus it is expected that the parameters updated in this study will improve the performances of the semi-active control system.

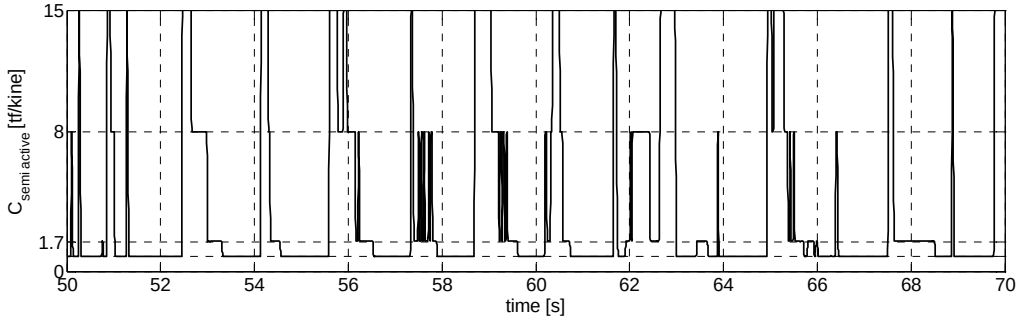

Fig. 12 Control gain signal

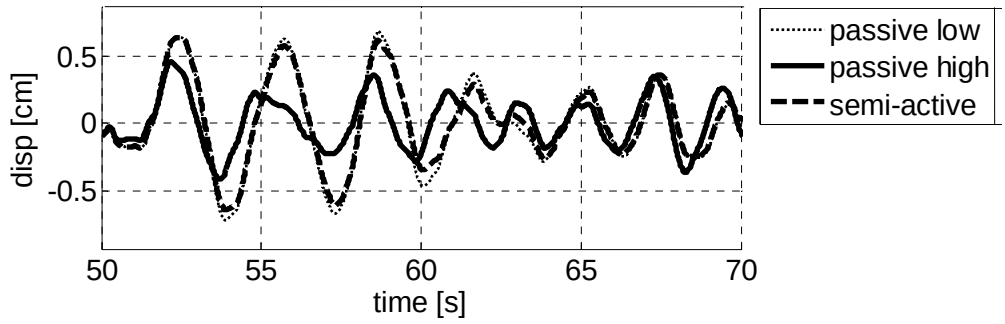

Fig. 13 Comparison of the base isolation layer relative displacement among three control methods

Table 6 Performances of control methods (black: worst, gray: intermediate, white: best)

Control	Isolation layer displacement [cm]		Isolation layer acceleration [cm/s^2]		7F acceleration [cm/s^2]	
	NS direction	EW direction	NS direction	EW direction	NS direction	EW direction
Low	0.68	0.75	2.89	3.46	4.33	5.17
High	0.42	0.47	3.39	4.03	5.57	5.91
Semi	0.66	0.68	2.72	3.41	4.13	4.72

CONCLUSIONS

The dynamic properties of the semi-active base isolation system of a university building were investigated based on observed records during the 2011 Great East Japan earthquake. The system parameters were identified using an ARX model, the N4SID method, and a direct optimization method to minimize an error in a response time history. A series of seismic response analyses were conducted, and it was confirmed that updated parameters gave more accurate estimations of the real behavior of the system compared to initial design ones. Consequently, it is expected that, in a near future, the semi-active control system can be efficiently updated with more accurate structural parameters to offer a better control of the building.

APPENDIX

Table 7 Initial structural parameters

Floor	Mass [kN]	Stiffness [kN/cm]		Damping coefficient [kN･s/cm]	
		NS direction	EW direction	NS direction	EW direction
RF	24500	11956	9996	100.80	80.487
7	20246	12936	11564	109.06	93.110
6	19962	14994	13818	126	111.26
5	19962	15778	15680	133.03	126.25
4	20090	17150	18130	144.60	145.98
3	19923	17248	18032	145.42	145.20
2	17894	17738	19796	149.56	159.40
1	24411	19796	27636	166.90	222.52
B1	33692	19796	22736	166.90	183.1
B2	48813	668.4	668.4	100.0	100.0

Table 8 Identified system characteristics of the entire building

Identification Method	Mode	NS direction			EW direction		
		Natural period [s]	Natural frequency [Hz]	Damping factor	Natural period [s]	Natural frequency [Hz]	Damping factor
Initial	1st	2.58	0.39	9%	2.56	0.39	7%
ARX		3.20	0.35	19%	3.10	0.36	24%
N4SID		3.23	0.31	18%	3.23	0.31	17%
Direct		3.25	0.31	14%	3.21	0.31	16%
Initial	2nd	0.77	1.29	9%	0.77	1.30	7%
ARX		0.68	1.47	17%	0.71	1.41	16%
N4SID		0.70	1.42	6%	0.72	1.38	8%
Direct		0.71	1.41	9%	0.72	1.38	8%

Table 9 Identified system characteristics of the superstructure

Identification Method	Mode	NS direction			EW direction		
		Natural period [s]	Natural frequency [Hz]	Damping factor	Natural period [s]	Natural frequency [Hz]	Damping factor
Initial	1st	1.32	0.76	2%	1.26	0.79	2%
ARX		1.10	0.91	5%	1.10	0.91	2%
N4SID		1.16	0.86	2%	1.11	0.90	8%
Direct		1.18	0.85	2%	1.20	0.83	2%
Initial	2nd	0.48	2.10	6%	0.47	2.11	5%
ARX		0.36	2.80	8%	0.37	2.70	4%
N4SID		0.47	2.12	7%	0.40	2.51	10%
Direct		0.44	2.27	7%	0.45	2.22	4%

REFERENCES

Mita, A. (2003). “Health Monitoring and Identification.” *Structural Dynamics for Health Monitoring*, Chap. 5, 84-96.

Van Overschee, P. and De Moor, B. (1994). “N4SID: Subspace Algorithms for the Identification of Combined Deterministic-Stochastic Systems.” *Automatica*, Vol. 30, No. 1, 75-93.

Yoshida, K. (2001). “First Building with Semi-Active Base Isolation.” *Journal of the Japan Society of Mechanical Engineers*, Vol. 104, No. 995, 698-702.